3-1-2023

Resolution of hepatic fibrosis after ZFN-mediated gene editing in the PiZ mouse model of human α1-antitrypsin deficiency

Yanfeng Li
Albert Einstein College of Medicine
Chandan Guha
Albert Einstein College of Medicine
Patrik Asp
Albert Einstein College of Medicine
Xia Wang
Albert Einstein College of Medicine
Tatyana L. Tchaikovskya
Albert Einstein College of Medicine

See next page for additional authors

Received: 27 May 2022 | Accepted: 21 December 2022

DOI: 10.1097/HC9.0000000000000070

ORIGINAL ARTICLE

OPEN

Resolution of hepatic fibrosis after ZFN-mediated gene editing in the PiZ mouse model of human α1-antitrypsin deficiency

Yanfeng Li[1] | Chandan Guha[2,3,4] | Patrik Asp[2,4] | Xia Wang[1] | Tatyana L. Tchaikovskya[1,4] | Kenneth Kim[5] | Matthew Mendel[5] | Gregory J. Cost[5] | David H. Perlmutter[6] | Namita Roy-Chowdhury[1,4,7] | Ira J. Fox[8] | Anthony Conway[5] | Jayanta Roy-Chowdhury[1,4,7]

[1]Department of Medicine, Albert Einstein College of Medicine, New York, New York, USA

[2]Department of Radiation Oncology, Albert Einstein College of Medicine, New York, New York, USA

[3]Department of Pathology, Albert Einstein College of Medicine, New York, New York, USA

[4]Marion Bessin Liver Research Center, Albert Einstein College of Medicine, New York, New York, USA

[5]Sangamo Therapeutics, Richmond, California, USA

[6]Department of Pediatrics, Washington University School of Medicine, St. Louis, Missouri, USA

[7]Department of Genetics, Albert Einstein College of Medicine, New York, New York, USA

[8]Department of Surgery, McGowan Institute for Regenerative Medicine, University of Pittsburgh Medical Center, Pittsburgh, Pennsylvania, USA

Correspondence
Jayanta Roy-Chowdhury, Albert Einstein College of Medicine, 1300 Morris Park Avenue, Bronx, NY 10461
Email: jayanta.roy-chowdhury@einsteinmed.edu

Abstract

Background: α1-antitrypsin deficiency is most commonly caused by a mutation in exon-7 of *SERPINA1 (SA1-ATZ)*, resulting in hepatocellular accumulation of a misfolded variant (ATZ). Human *SA1-ATZ*-transgenic (PiZ) mice exhibit hepatocellular ATZ accumulation and liver fibrosis. We hypothesized that disrupting the *SA1-ATZ* transgene in PiZ mice by *in vivo* genome editing would confer a proliferative advantage to the genome-edited hepatocytes, enabling them to repopulate the liver.

Methods: To create a targeted DNA break in exon-7 of the *SA1-ATZ* transgene, we generated 2 recombinant adeno-associated viruses (rAAV) expressing a zinc-finger nuclease pair (rAAV-ZFN), and another rAAV for gene correction by targeted insertion (rAAV-TI). PiZ mice were injected i.v. with rAAV-TI alone or the rAAV-ZFNs at a low (7.5×10^{10}vg/mouse, LD) or a high dose (1.5×10^{11}vg/mouse, HD), with or without rAAV-TI. Two weeks and 6 months after treatment, livers were harvested for molecular, histological, and biochemical analyses.

Results: Two weeks after treatment, deep sequencing of the hepatic *SA1-ATZ* transgene pool showed 6% ± 3% or 15% ± 4% nonhomologous end joining in mice receiving LD or HD rAAV-ZFN, respectively, which increased to 36% ± 12% and 36% ± 12%, respectively, 6 months after treatment. Two weeks postinjection of rAAV-TI with LD or HD of rAAV-ZFN, repair by targeted insertion occurred in 0.10% ± 0.09% and 0.25% ± 0.14% of *SA1-ATZ* transgenes,

Abbreviations: AAT, α_1-antitrypsin; ATD, α_1-antitrypsin deficiency; Gli2, glioblastoma-2; HD, high dose; HRD, homologous recombination donor strand; Ihh, Indian hedgehog; rAAV-ZFN, recombinant adeno-associated viruses (rAAV) expressing zinc-finger nuclease; rAAV-TI, rAAV designed to provide a wild-type homologous recombination donor strand for gene correction by targeted insertion; Shh, sonic hedgehog; *SA1-ATZ*, mutant human *SERPINA1* transgene-expressing mutant ATZ; TI, targeted integration; TAZ/WWTR1, transcriptional coactivator with PDZ-binding motif; ZFN, zinc-finger nuclease.

Anthony Conway and Jayanta Roy-Chowdhury are co-communicating authors.

Supplemental Digital Content is available for this article. Direct URL citations appear in the printed text and are provided in the HTML and PDF versions of this article on the journal's website, www.hepcommjournal.com.

respectively, which increased to 5.2% ± 5.0% and 33% ± 13%, respectively, 6 months after treatment. Six months after rAAV-ZFN administration, there was a marked clearance of ATZ globules from hepatocytes, and resolution of liver fibrosis, along with reduction of hepatic TAZ/WWTR1, hedgehog ligands, Gli2, a TIMP, and collagen content.

Conclusions: ZFN-mediated *SA1-ATZ* transgene disruption provides a proliferative advantage to ATZ-depleted hepatocytes, enabling them to repopulate the liver and reverse hepatic fibrosis.

INTRODUCTION

The serine protease inhibitor glycoprotein, α1-antitrypsin (AAT), encoded by *SERPINA1,* is the most abundant protease inhibitor in the plasma and is expressed primarily in hepatocytes. AAT protects pulmonary connective tissue from excessive degradation by inhibiting neutrophil elastase activity.[1] Disease-producing mutations of *SERPINA1* cause lung and/or liver disease in 3.4 million individuals worldwide.[2] In its classic form, AAT-deficiency disease (ATD) results from homozygous inheritance of a mutant *SERPINA1* gene (*SA1-ATZ*), expressing a lysine342glutamate-substituted AAT, which is misfolded, and prone to accumulation, polymerization, and aggregation within hepatocytes.[3,4] On the basis of the difference in electrophoretic mobility, this mutant AAT is termed ATZ, whereas the normal allele is termed ATM. ATZ is secreted inefficiently, reducing its plasma levels to ~15% of normal, leading to panacinar pulmonary emphysema due to uninhibited leukocyte elastase activity.[3] On the other hand, hepatocyte stress caused by the accumulation of ATZ results in liver injury. Genetic and/or environmental modifiers protect 80%–90% of subjects homozygous for ATZ from severe liver disease. In the remaining 10%–20%, the liver phenotype ranges from mild liver disease to cirrhosis and hepatoma.[5] Although many patients with ATD liver disease present during childhood, 77% of ATD patients receiving liver transplantation in the US are adults (peak age 50–64 y).[6]

Intravenous infusion of pooled human plasma AAT or recombinant human AAT retards ATD progression in a subset of patients with moderate emphysema.[7] However, this lifelong therapy is expensive and does not affect the hepatic manifestation of ATD. Although prophylactic liver transplantation could potentially cure both the liver and lung phenotype, this formidable procedure commits the patient to long-term immunosuppression and is reserved for patients with acute or chronic liver failure, advanced cirrhosis, or hepatoma. Hepatocyte transplantation has been used to treat a variety of inherited metabolic liver diseases.[8] As the liver/body weight ratio is maintained within tight limits by physiological mechanisms, transplanted hepatocytes that engraft as single cells or small clusters do not proliferate significantly, except in diseases associated with loss of hepatocyte mass, such as in fumarylacetoacetate hydrolase deficiency (model of human tyrosinemia-1)[9] or to a modest degree in ATP7B-deficient Long-Evans cinnamon rats (model of Wilson disease).[10] However, as there is no major loss of hepatocyte mass in most inherited metabolic liver diseases, the engrafted hepatocytes do not proliferate significantly, whereby the metabolic abnormality is only partially ameliorated.

PiZ mice are transgenic for human *SA1-ATZ* and are a model of ATD liver disease. We previously reported that although the liver mass remains normal in PiZ mice, hepatocellular stress from ATZ accumulation results in a competitive disadvantage to host hepatocytes, permitting transplanted wild-type hepatocytes to proliferate by progressively replacing the host hepatocytes (over a period of 6 months, without changing the liver mass.[11] As hepatocytes of untreated PiZ mice can survive, divide and maintain the liver mass,[12] our finding of liver repopulation by proliferation of a small number of engrafted hepatocytes (~1% of liver mass) through attrition of the PiZ host hepatocytes provided evidence for by cell competition.[11] Importantly, liver repopulation by wild-type hepatocytes reversed the progression of liver fibrosis in recipient PiZ mice. Subsequently, Borel et al[13] reported that transplanted wild-type human hepatocytes could also repopulate the livers of immunodeficient ATZ-transgenic mice. These studies led to our hypothesis that if a small fraction of hepatocytes of PiZ mice could be relieved of the ATZ load by gene editing, such cells would proliferate preferentially, competitively replacing the ATZ-expressing hepatocytes. This was supported by experiments in which ATZ expression was suppressed in a fraction of PiZ mouse hepatocytes by expressing a synthetic miRNA[14] or targeting hSERPINA1 by CRISPR-Cas9 expressed through adenoviral delivery.[15]

In the present study, we used a recombinant adeno-associated virus (rAAV) pair expressing zinc-finger nucleases (ZFN) from a hepatocyte-specific promoter (rAAV-ZFN) in PiZ mice to generate a targeted DNA break near the mutation site in the *SA1-ATZ* transgene, and another rAAV to provide a DNA sequence for

targeted insertion (rAAV-TI) to correct the mutation through homologous recombination. The proportion of ATZ genomes undergoing nonhomologous end joining (NHEJ) or homologous recombination was determined by deep sequencing of genomic DNA 2 weeks and 6 months after rAAV injection. The results showed NHEJ or targeted integration (TI) in a small percentage of the *SA1-ATZ* transgene 2 weeks after treatment, which increased markedly 6 months after treatment, without a change in the liver/body weight ratio. Importantly, repopulation by the *SA1-ATZ* gene-disrupted hepatocytes resulted in a marked resolution of hepatic fibrosis. Activation of HSC through hedgehog ligands secreted by stressed or inflamed hepatocytes has been implicated in liver fibrosis,[16,17] and hepatic transcriptional coactivator with PDZ-binding motif (TAZ/WWTR1) is known to induce hedgehog proteins.[18] Therefore, to elucidate the mechanism of fibrosis resolution in PiZ mice, we quantified the hepatic contents of TAZ/WWTR1 and hedgehog proteins, as well as downstream effectors of hedgehog signaling of HSCs, namely glioma-associated protein (Gli2) and tissue inhibitor of metaloproteinase (TIMP).[19]

Our findings indicate that progressive repopulation of the PiZ mouse liver by *SA1-ATZ* transgene-disrupted hepatocytes resulted in the reduction of hepatic content of TAZ and hedgehog proteins, as well as the downstream effectors of hedgehog signaling Gli2, TIMP, and collagen, which could explain the extensive amelioration of hepatic fibrosis.

METHODS

Animals

PiZ mice carrying genomic integrations of human *SA1-ATZ* gene[20] were backcrossed with wild-type C57Bl/6 mice (Jackson Laboratory) and were bred and maintained at Albert Einstein College of Medicine on mouse lab chow in climate-controlled rooms at 12-hour light/dark cycles. Both female and male mice were used. Control wild-type C57Bl/6 mice, purchased from Jackson Laboratory, were cohoused with the PiZ mice. Tail vein injections were performed between 10 and 11 AM under isoflurane inhalation anesthesia. All animal experiments were performed with the approval of the Animal Care and Use Committees of Albert Einstein College of Medicine and the University and were within the guidelines for the humane care of laboratory animals.

rAAV-ZFN and rAAV-TI

To generate a dsDNA break in the genomic regions flanking the PiZ mutation, 2 rAAVs (AAV2/8, containing AAV2 ITRs and AAV8 capsid) were generated to express ZFNs from a hepatocyte-specific promoter consisting of the apolipoprotein E locus control region, human AAT promoter, a portion of intron-A of human coagulation factor IX, 3′-untranslated region, and a bovine growth hormone polyadenylation signal.[21] ZFNs were designed with Fok1 nuclease monomer fused at the carboxy terminals of the zinc-finger proteins. When the 2 ZFN molecules home at their respective DNA sequence recognition sites on the 2 complementary DNA strands, the Fok1 monomers dimerize, generating an active nuclease (Figure 1A). For homology-directed correction of the pathogenic mutation on exon-7 of *SA1-ATZ*, rAAV-TI was designed by replacing the AAV2 genome with a segment of the wild-type human *SERPINA1* gene consisting of left and right homology arms, ~1 kb each, flanking the mutation site, between the AAV2 ITRs. Two silent mutations were inserted into the homologous recombination donor to prevent recleavage by ZFN.

Experimental groups

Five experimental groups of 6-week-old PiZ mice (n = 6) were infused through the tail vein as follows: group 1: rAAV-TI (1.5×10^{12} viral genomes, vg) alone; group 2: rAAV-ZFN pair low dose (LD, 7.5×10^{10}vg); group 3: rAAV-ZFN pair high dose (HD, 1.5×10^{11}vg); group 4: rAAV-ZFN pair at LD plus rAAV-TI (1.5×10^{12}vg); and group 5: rAAV-ZFN pair at HD plus rAAV-TI (1.5×10^{12}vg). The treatment groups and the PiZ and C57/Bl6 control groups are described in Table 1.

Quantification of genome editing

A 2.1 kb segment *SA1-ATZ* was amplified by PCR, and a ~240-bp segment of the amplicon was reamplified for Illumina next-generation sequencing. Subsequently, Illumina adaptor and barcode PCRs were performed, and the purified amplicons were sequenced using Illumina Miseq for the quantification of sequences containing insertions and deletions (*indel*s), as well as TI of the gene correction donor.

For additional materials and methods, please see Supplementary Materials and Methods, http://links.lww.com/HC9/A163.[22,24]

RESULTS

The proportion of *SA1-ATZ* transgene-edited hepatocytes increased over time in the PiZ mouse livers

Figure 1B (i) shows the proportion of total *indel*-containing *SA1-ATZ* transgenes (NHEJ) in PiZ mouse livers as a

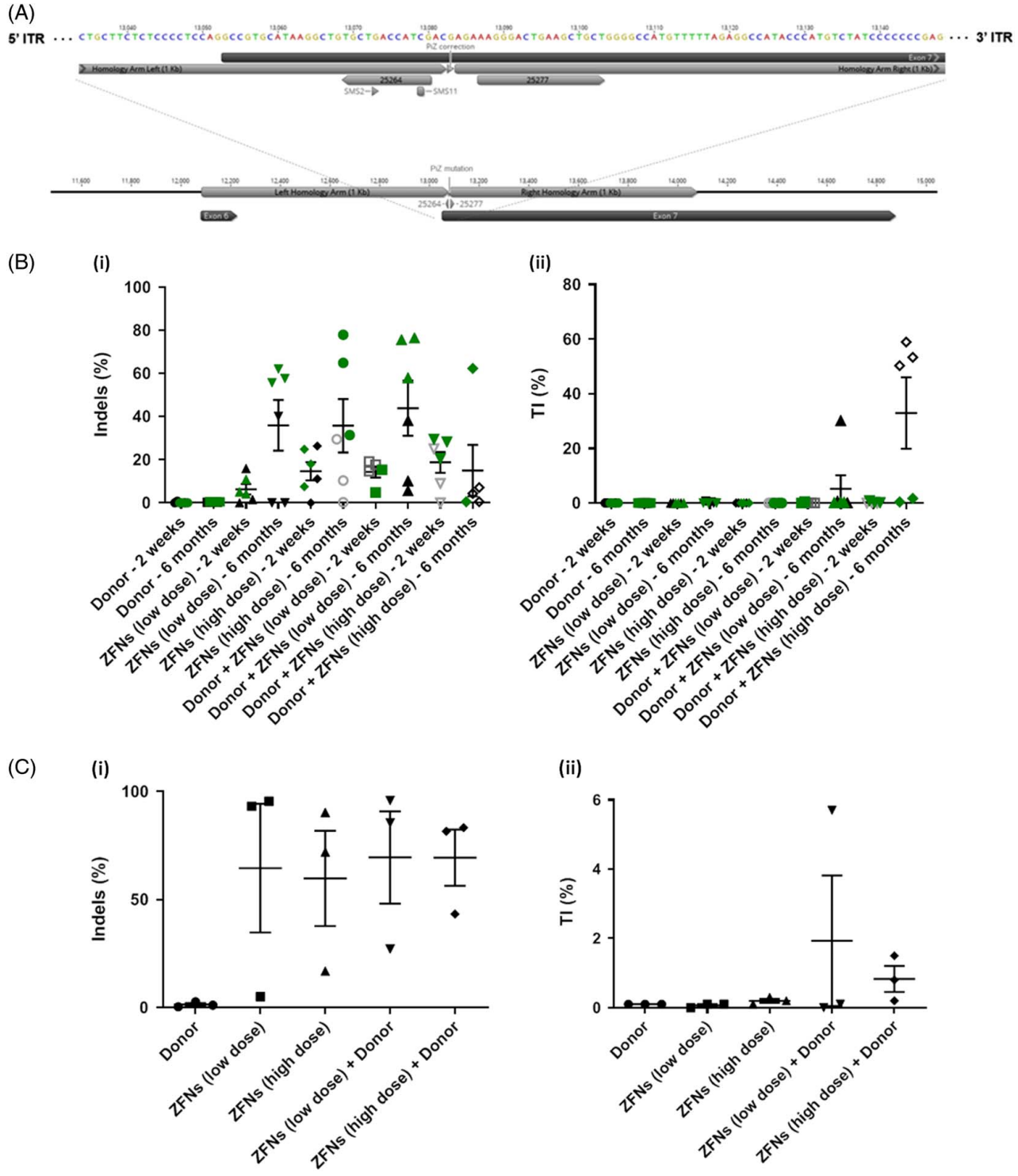

percentage of total transgene content. In group 1, (rAAV-TI only), the transgene editing was negligible both 2 weeks and 6 months after injection. In group 2, which received rAAV-ZFN pair at a low dose (LD, 7.5×10^{10}vg) without rAAV-TI, *indel* was present in $6\%\pm3\%$ (mean $\pm$ SEM) of *SA1-ATZ* transgenes at 2 weeks but increased to $36\%\pm12\%$ at 6 months after rAAV injection. When a higher dose (HD, 1.5×10^{11}vg) of the rAAV-ZFN pair was used (group 3), *indel*s increased from $15\%\pm4\%$ at 2 weeks to $36\%\pm12\%$ at 6 months. When rAAV-TI was added to LD rAAV-ZFN (group 4), $14\%\pm3\%$ and $44\%\pm13\%$ of *SA1-ATZ* contained *indels* 2 weeks and 6 months after treatment, respectively. In group 5, which received HD rAAV-ZFN (1.5×10^{11}vg) with rAAV-TI, the percentage of indel-containing *SA1-ATZ* was $19\%\pm5\%$ and $15\%\pm12\%$ at 2 weeks and 6 months, respectively. There was a trend toward an increase in the proportion of *indel*-containing *SA1-ATZ* transgenes between 2 weeks and

FIGURE 1 Editing of the pathogenic mutation in the human SERPINA1 transgene *(SA1-ATZ)*: (A) Gene correction schematic. (i) Recombinant AAV for correcting the pathogenic ATZ mutation in the human *SA1-ATZ* transgene in PiZ mice by homology-directed targeted insertion (rAAV-TI) was designed with the wild-type human SERPINA1 sequence. Left and right homology arms ~1 kb each were used to promote homology-directed repair at the ZFN cut site (between 25264 and 25277) near the PiZ mutation. Two silent mutations (SMS2 and SMS11) were introduced into 1 of the 2 ZFN binding sites (25264 and 25277) encoded within the AAV donor construct to prevent ZFN binding and recleavage after gene correction. These silent mutations do not change the amino acid coding sequence within exon-7 of the *SA1-ATZ* transgene, but alter the DNA sequence of the ZFN binding site, which prevents binding of the specific sequence-targeted 25264 ZFN. The rAAV-TI also consists of inverted terminal repeats (ITRs) at the 5′ and 3′ of the packaged viral genome. (ii) Human SA1-ATZ locus shown with ZFN binding sites and AAV gene correction donor homology arm sequences. (B) Genomic editing of human SA1-ATZ transgene in PiZ mouse livers 2 weeks and 6 months after injection of rAAVs. (i) rAAV-TI gene correction donor and/or rAAV-ZFN pair, encoding human SERPINA1-targeted ZFN expression constructs (25264 and 25277) were i.v. injected into PiZ mice at a constant dose of rAAV-TI (1.5×10^{12}vg) and/or high (HD, 1.5×10^{11}vg) or low doses (LD, 7.5×10^{10}vg) of rAAV-ZFN. Although there was a trend of increasing *indel*s from 2 weeks to 6 months for most ZFN-treated groups, differences in *indel*s between the AAV-treated groups were not statistically significant. (ii) Targeted integration (TI) of the gene correction construct was observed only in groups receiving the donor rAAV-TI plus rAAV-ZFNs at 6 months after treatment. Gene correction occurred to a greater extent in the HD rAAV-ZFN group. $p = 0.0087$ comparing TI at the 2-week versus 6-month time points in rAAV-TI + rAAV-ZFNs (high dose) groups. $p = 0.0303$ comparing TI for low dose and high-dose Donor + ZFNs 6-month posttreatment groups. Green data points indicate animals from cohort 1; all other data points are from cohort 2. Error bars represent SE of the mean (SEM). Mann-Whitney unpaired nonparametric analysis was used to calculate statistical significance. (C) Genomic editing of human SA1-ATZ transgene in hepatocytes isolated from PiZ mouse livers at 2 weeks and 6 months after injection of rAAVs. (i) rAAV-TI and/or rAAV-ZFNs encoding ZFNs targeting the *SA1-ATZ* transgene (25264 and 25277) were injected i.v. into PiZ mice at a constant dose of rAAV donor (1.5×10^{12}vg/mouse) and/or a low or high dose of rAAV-ZFNs (7.5×10^{10} vg/mouse or 1.5×10^{11} vg/mouse, respectively). Six months after treatment, hepatocytes were isolated by collagenase perfusion and purified by differential centrifugation for subsequent genome editing analysis. Difference in *indel* frequency observed between any of the rAAV-ZFN-treated groups was not statistically significant. (ii) Targeted integration (TI) of the gene correction construct was observed at higher levels only in the rAAV-TI plus rAAV-ZFN groups, although the difference in frequency of TI observed between groups did not reach statistical significance because of the limited sample size. Mann-Whitney unpaired nonparametric analysis was used to calculate statistical significance. Abbreviations: ZFN, zinc-finger nuclease.

6 months after injection of rAAV-ZFN, with or without rAAV-TI. Particularly in the LD groups (2 and 4), the average percentage of indel-containing *SA1-ATZ* transgenes increased 3 to 6-fold between 2-week and 6-month time points. However, because of the high SE of means, these differences did not reach statistical significance.

Indel quantification in liver homogenates reflects hepatocytes and nonparenchymal cells, but the latter are not expected to undergo DNA break as the ZFNs are expressed from a hepatocyte-specific promoter. Therefore, in 3 additional mice, we isolated hepatocytes 6 months after treatment by collagenase perfusion and purified hepatocytes by differential centrifugation to >98% homogeneity. As shown in Figure 1C, injection of rAAV-TI alone (group 1), resulted in *indel*s in only $1.4\% \pm 0.6\%$ (mean ± SEM) of the transgenes. In contrast, in all groups receiving rAAV-ZFN, percentages of transgene NHEJ-containing SA1-ATZ were high (65 ± 26, 60 ± 19, 70 ± 19, and 69 ± 11, in groups 2, 3, 4, and 5, respectively), which were 42% to 50%-fold higher than that found with rAAV-TI alone (group 1) ($p < 0.02$). The difference among that had received rAAV-ZFN (groups 2–5) was small and not statistically significant. The results indicate a marked increase in the proportion of the *SA1-ATZ*-disrupted hepatocytes over that of the transgene-expressing hepatocytes. Notably, the repopulation did not result in a significant change in the liver/body weight ratio (Supplemental Figure S1, http://links.lww.com/HC9/A162), indicating that proliferation of the transgene-disrupted hepatocytes was commensurate with the loss of transgene-expressing host hepatocytes.

TABLE 1 Experimental design

Experimental groups	rAAV-TI (HR donor)	rAAV-TI dose (genome copies)	rAAV-TI day of injection	rAAV-ZFN pair	rAAV-ZFN dose (genome copies)	rAAV-ZFN day of injection	Blood sampling days	Day of sacrifice after injection
1	SMS24	1.5×10^{12}	0	—	—	—	3; 180	14; 180
2	—	—	—	25264:25277	0.75×10^{12}	6	3; 180	14; 180
3	—	—	—	25264:25277	1.5×10^{12}	6	3; 180	14; 180
4	SMS24	1.5×10^{12}	0	25264:25277	0.75×10^{12}	6	3; 180	14; 180
5	SMS24	1.5×10^{12}	0	25264:25277	1.5×10^{12}	6	3; 180	14; 180
Control groups:	—	—	—	—	—	—	—	—
PiZ control	PBS	—	0	—	—	—	3;180	14; 180
C57/Bl6	None	—	—	—	—	—	3;180	—

Experimental groups: Five experimental groups of 6-week-old PiZ mice, 6 in each group, were infused by means of the tail vein either the rAAV-TI alone or 2 different doses of the rAAV-ZFN pair or 2 different doses of the rAAV-ZFN pair plus the rAAV-TI.

Mutation in *SA1-ATZ* transgene was corrected only when rAAV-TI was added to rAAV-ZFN

Figure 1B (ii) shows the percentage of *SA1-ATZ* transgenes that underwent gene correction by targeted insertion of the donor DNA (TI). As expected, TI was observed only in groups receiving both rAAV-TI and rAAV-ZFN. Six months after treatment, in group 4 (rAAV-TI plus low-dose rAAV-ZFN) and group 5 (rAAV-TI plus high-dose rAAV-ZFN), percentages of *SA1-ATZ* transgenes undergoing gene correction were $5.2\% \pm 5.0\%$ and $33\% \pm 13\%$, respectively ($p = 0.0303$). The differences between the 2-week and 6-month time points in both these groups were also statistically significant ($p = 0.0087$). In 50% of the mice in group 5, 50%–60% of the *SERPINA1-PiZ* transgenes had undergone gene correction by TI.

rAAV-ZFN treatment reduced the number of PiZ globule-containing hepatocytes 6 months after treatment

Polymerized PiZ globules in hepatocytes of PiZ mice were visualized by Periodic acid-Schiff staining of liver cryosections after glycogen digestion by diastase treatment (Figure 2A). Percentage of globule-containing cells was determined by ImageJ analysis (Figure 2B). In the liver of untreated PiZ mice, $85\% \pm 10\%$ (mean $\pm$ SEM) of the hepatocytes contained PiZ globules at the age of 8 weeks, but the percentage declined spontaneously to 60%+8% at the age of 30 weeks. In PiZ mice receiving rAAV-TI only (group 1), 2 weeks and 6 months after treatment, percentages of globule-containing hepatocytes were similar to those in age-matched PiZ mouse controls. In all groups that received rAAV-ZFN (groups 2–5), the proportion of globule-containing cells was not significantly different from age-matched control PiZ mice 2 weeks after treatment. However, 6 months after treatment, the percentage of globule-containing cells was markedly reduced ($p < 0.02$, Figure 2B). Six months after treatment, the differences between group 1 and groups 2–5 were also significant ($p < 0.02$).

rAAV-ZFN treatment reduced serum total human AAT levels 6 months after treatment

Serum human AAT concentrations in PiZ mice did not decline significantly between 2-week and 6-month time points after injection of rAAV-TI alone (group 1) (Figure 2C). In contrast, in all groups receiving rAAV-ZFN, at low (LD) or high (HD) dose, with or without rAAV-TI, serum human AAT levels declined significantly 6-month posttreatment from the 2-week levels (*, $p < 0.02$). As the serum human AAT is the sum of the ATZ expressed from the *SA1-ATZ* transgene and possibly any human ATM expressed from the transgene corrected by targeted insertion, the results are consistent with a higher frequency of transgene disruption by NHEJ than that of gene correction by targeted insertion, as shown in Figure 1B, C.

rAAV-ZFN treatment markedly reduced liver fibrosis

In contrast to the age-related decline of the proportion of globule-containing hepatocytes in PiZ mouse livers, liver fibrosis advances with age. Therefore, we determined the effect of *SA1-ATZ* transgene editing in PiZ mice on liver fibrosis 2 weeks and 6 months after treatment. Cryopreserved liver sections were stained with Sirius red (Figure 3A, B) and paraffin sections of formaldehyde-fixed liver tissues were stained with Masson trichrome (Figure 3D) to evaluate liver fibrosis. Collagen deposition was quantified by ImageJ analysis for the Sirius red (Figure 3C) and Masson trichrome (Figure 3E, respectively). In PBS-treated control PiZ mice, both staining methods showed significantly greater collagen staining 2-week postinjection than in age-matched (8-week old) congeneic wild-type C57/Bl6 control mice ($p < 0.02$, Figure. 3C, E). In the PBS-treated PiZ mice, the collagen content increased $>$2-fold over wild-type mice 6-month postinjection (age 30 weeks, $p < 0.02$). At this time point, some areas of the liver exhibited regenerative nodules consisting of groups of hepatocytes completely surrounded by collagen strands (Figure 3B). In PiZ mice receiving rAAV-TI only (group 1), liver collagen content was similar to PBS-treated PiZ mice, both 2 weeks (age 8 wk) and 6 months (age 30 wk) after treatment (Figure 3A, C, D, E). In contrast, in all groups receiving rAAV-ZFN (groups 2–5), fibrosis was significantly reduced 6 months after treatment ($p < 0.02$, Figure 3A, C–E). In groups receiving HD of rAAV-ZFN, without (group 3) or with rAAV-TI (group 5), collagen strands were markedly reduced 6 months after treatment (age 30 wk) to levels similar to that in age-matched C57/Bl6 mice (Figure 3E), and regenerative nodules were absent (Figure 3B). Western blot for collagen-1 (Figure 4A, B) confirmed the increase in collagen content with age in control PiZ mice and marked reduction of collagen content in all groups receiving the rAAV-ZFN with or without rAAV-TI 6-month posttreatment ($p < 0.01$).

Hepatic Indian hedgehog and Shh contents were reduced 6 months after rAAV-ZFN administration

Signaling of HSCs by hedgehog ligands secreted by stressed hepatocytes is being recognized to be pivotal in liver fibrosis in several liver diseases,[16] including

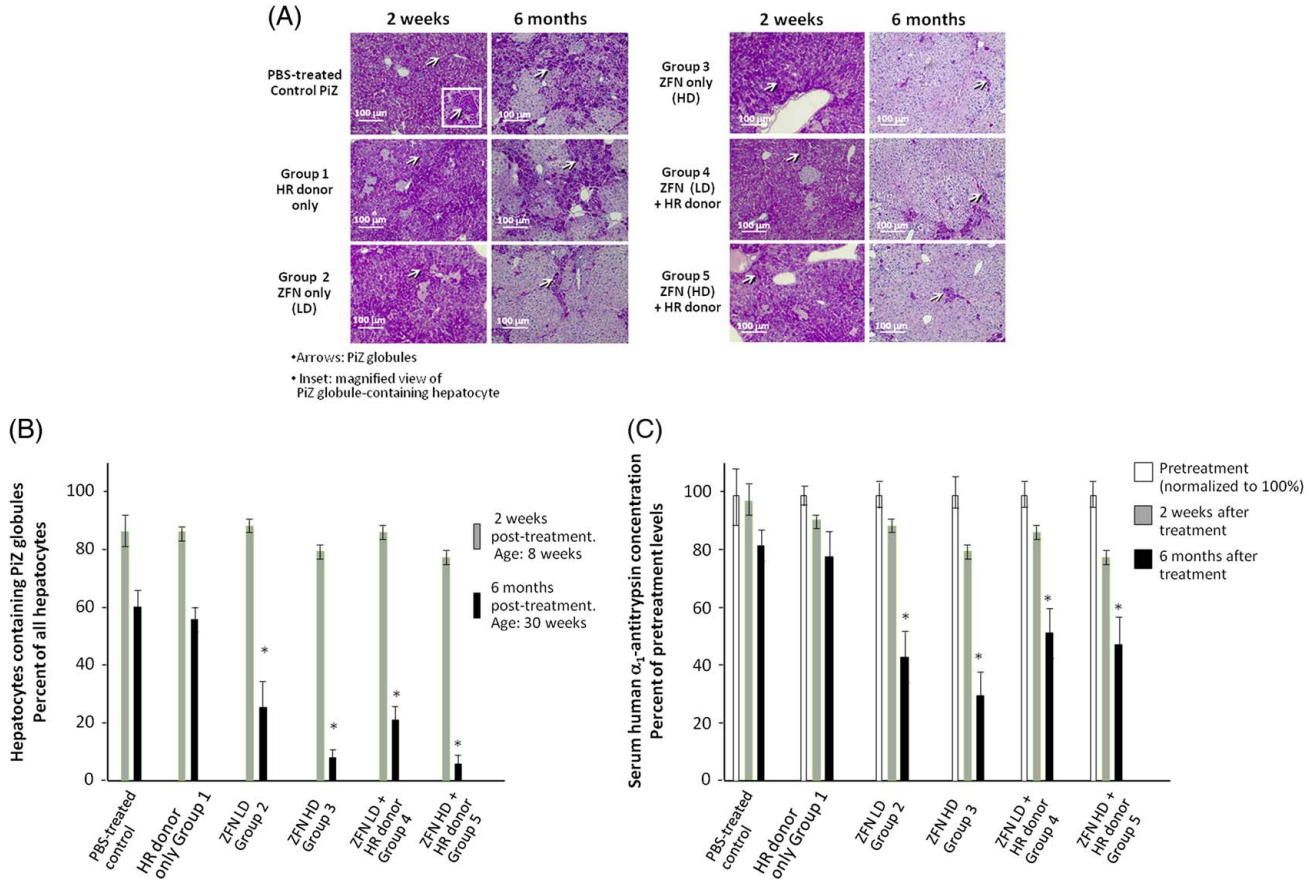

FIGURE 2 Human SERPINA1 in liver and serum. Globules of polymerized mutant human SERPINA1 in PiZ mouse hepatocytes. Six-week-old PiZ mice were injected with the different combinations of rAAV as listed in Table 1 (6 mice per group) and sacrificed 2 weeks or 6 months later for histological and serological analysis. Age-matched PBS-injected PiZ mice were used as control. (A) Periodic acid-Schiff (PAS) staining: liver cryosections were treated with diastase to deplete glycogen and then polymerized PiZ globules were visualized by PAS staining (arrows). Inset shows a magnified globule-containing hepatocyte. (B) Quantification of PiZ globule-containing hepatocytes: percentage of globule-containing hepatocytes was determined by counting at least 1600 cells in each section. Bars represent means ± SEM. Note that in PBS-treated control PiZ mice, the proportion of globule-containing cells decreased in the interval between 2 weeks and 6 months after injection. Similar degree of reduction of globule-containing cells occurred in mice receiving rAAV-TI only (group 1) between 2 weeks and 6 months after injection. In contrast, there was significantly greater reduction in the percentage of globule-containing cells between 2 weeks and 6 months in all groups receiving rAAV-ZFN at low ($7.5 \times 10^{\wedge 10}$ vg/mouse, LD) or high ($1.5 \times 10^{\wedge 11}$vg/mouse, HD) dose without (groups 2 and 3) or with (groups 4 and 5) rAAV-TI. (*Significantly different from values in PBS-injected PiZ mice 6 months after injection, $p < 0.02$). Addition of the rAAV-TI did not significantly enhance the reduction of the globule-containing cells over administration of rAAV-ZFN alone. (C) Serum total human AAT concentrations: AAT levels in the PiZ mouse sera were determined by ELISA using a human AAT-specific antibody, before rAAV administration and 2 weeks and 6 months after treatment. Injection of rAAV-TI alone (group 1) did not significantly reduce serum human PiZ levels between 2 weeks and 6 months after treatment. In contrast, serum human PiZ levels were significantly reduced (*$p < 0.02$) at the 6-month time point compared with the 2-week levels in all recipients of rAAV-ZFN, both at the low (LD) or high (HD) dose, with or without rAAV-TI. Arrows: PiZ globules. Inset: magnifies view of PiZ globule-containing hepatocyte. Abbreviations: HR, homologous recombination; ZFN, zinc-finger nuclease.

ATD and nonalcoholic steatohepatitis. We determined hepatic levels of the signaling proteins, Indian hedgehog (Ihh) (Figure 5A, B) and sonic hedgehog (Shh) (Figure 5C, D) by western blot analysis. In 30-week-old PiZ mice, hepatic Ihh and Shh levels were increased 5- to 6-fold over those in age-matched wild-type controls. In age-matched PiZ mice 6-month postinjection of rAAV-TI alone, there was no significant reduction of Ihh or Shh content compared with control PBS-treated PiZ mice. In contrast, in all PiZ mice receiving rAAV-ZFN, with or without the rAAV-TI, both Ihh and Shh levels declined to near normal 6-month posttreatment (Figure 5A–D).

TAZ/WWTR1 was reduced 6 months after rAAV-ZFN administration

TAZ is a transcriptional cofactor that induces Ihh expression in hepatocytes, leading to hepatic inflammation and fibrosis under certain conditions of hepatocellular stress.[18] Therefore, we quantified hepatic TAZ content by western blot analysis/densitometry. Hepatic TAZ content was low in 30-week-old control wild-type mouse livers, but was elevated over 6-fold in age-matched PBS-treated control PiZ mice (Figure 5E, F). Six weeks after treatment, TAZ content was not significantly changed in mice receiving

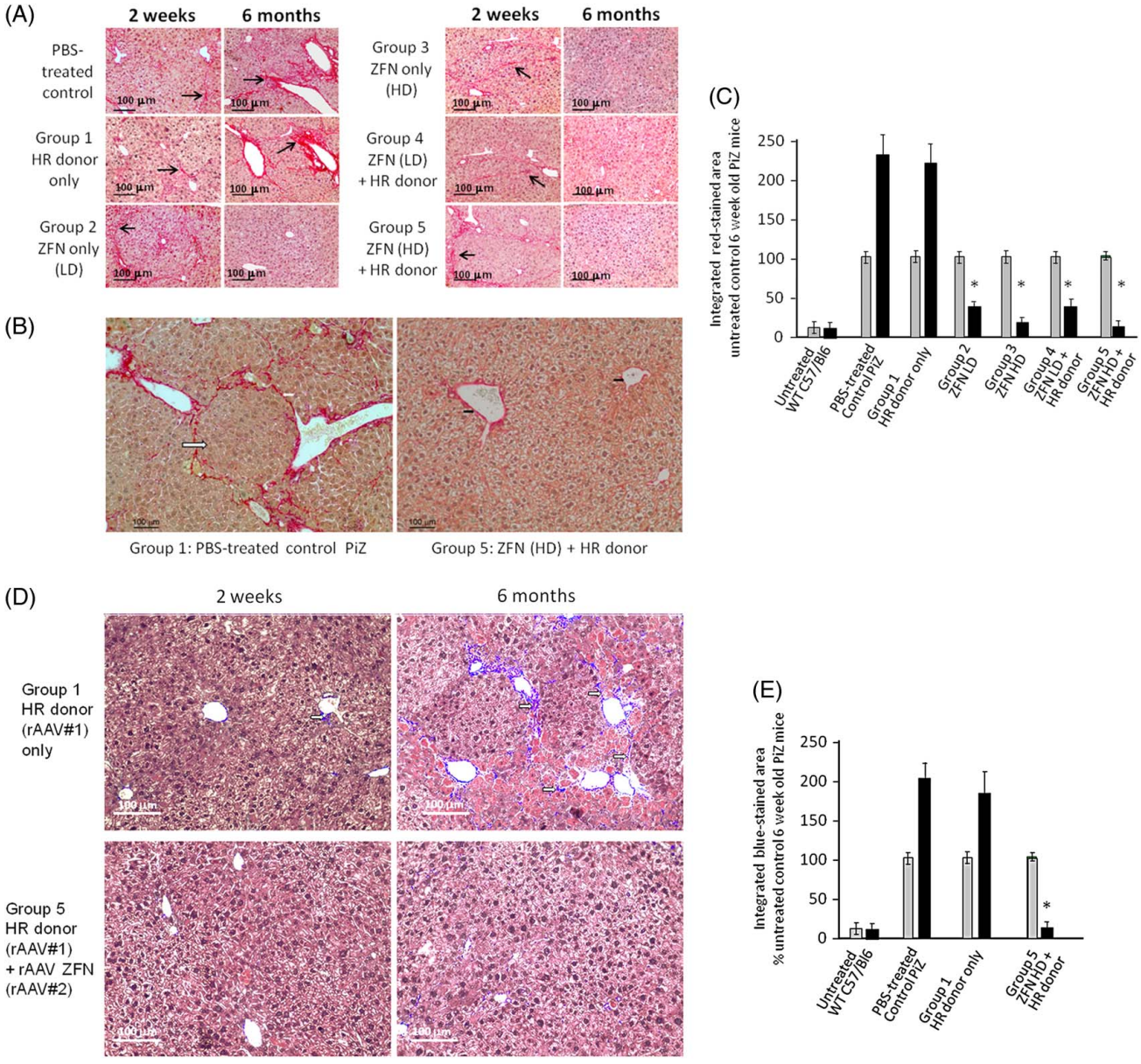

FIGURE 3 Histological evaluation of liver fibrosis: The extent of liver fibrosis was evaluated by staining liver paraffin sections with 2 different methods: Sirius red and Masson trichrome. The experimental and control groups are as in Table 1. (A) Sirius red staining: representative liver sections from PBS-treated PiZ mice and mice from each of the 5 experimental groups at indicated time points after injection are shown. Note that without treatment, liver fibrosis increases with age in PiZ mice, as shown in the PBS-stained control. (B) left panel: Sirius red–stained liver section from a 30-wk old PBS-treated control PiZ mouse showing a regenerative nodule consisting of groups of hepatocytes surrounded by collagen strands. Right panel: liver section from 30-week-old PiZ mouse from group 5, which had received treatment 6 months before the analysis, showing no evidence of regenerative nodule formation. (C) Quantification of the sirius red–stained collagen fibers by ImageJ analysis. Gray bars, 2 weeks after treatment; solid black bars, 6 months after treatment. Liver sections from untreated normal C57/Bl6 mice were analyzed as normal controls. *Significantly different from values in PBS-injected PiZ mice 6 months after injection, $p < 0.02$. (D). Masson trichrome staining: representative liver sections from values in PBS-treated PiZ mice and mice from experimental groups 1 and 5 at indicated time points after injection are shown. (E) Quantification of the Masson trichrome-stained collagen fibers (blue) by ImageJ analysis. Gray bars, 2 weeks after treatment; solid black bars, 6 months after treatment. Liver sections from untreated normal C57/Bl6 mice were analyzed as normal controls. *Significantly different from values in PBS-injected PiZ mice 6 months after injection, $p < 0.02$). Abbreviations: HD, high dose; HR, homologous recombination; rAAV, recombinant adeno-associated viruses; WT, wild type; ZFN, zinc-finger nuclease.

rAAV-TI only (group 1). In contrast, in PiZ mice receiving rAAV-ZFN, without (group 3) or with (group 5) rAAV-TI, TAZ content was significantly reduced compared with age-matched PiZ mouse controls ($p < 0.02$).

Hepatic Gli2 content was reduced 6 months after rAAV-ZFN administration

Hedgehog signaling is mediated by the stabilization and nuclear localization of proteins of the glioma family

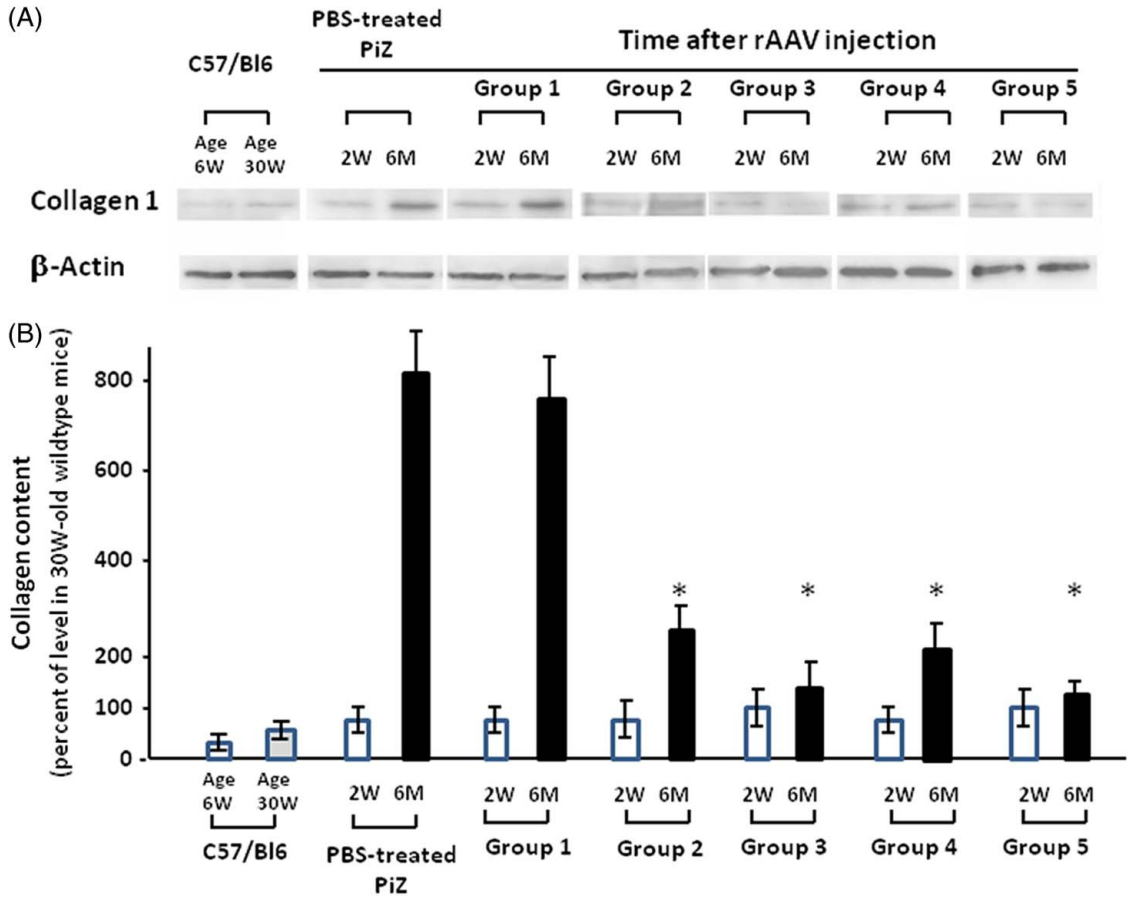

FIGURE 4 Western blot analysis of hepatic collagen. (A) Western blot analysis for collagen-1: Western blot analysis was performed on liver homogenates of PiZ mice in all 5 experimental groups and PBS-injected PiZ mouse controls 2 and 6 weeks after injections. Livers from age-matched wild-type C57/Bl6 mice were also analyzed. Representative western blots for collagen-1 are shown along with β-actin as loading control. B. Quantification of collagen-1: hepatic collagen-1 contents were determined by scanning the western blot bands and are shown as percentage of the collagen-1 content in 30-week-old wild-type C57/Bl6 mouse livers (means ± SEM, 6 mice in each group). *Significantly different from values in PBS-injected PiZ mice 6 months after injection, $p < 0.02$). Abbreviations: rAAV, recombinant adeno-associated viruses.

(Gli).[17] Therefore, we determined hepatic Gli2 content by western blot analysis/densitometry. Hepatic Gli2 content was ~3-fold higher in 30-week-old PiZ mice than in age-matched wild-type controls (Figure 6A, B). Gli2 content was not significantly changed in PiZ mice receiving the rAAV-TI only (group 1), 6-month posttreatment. In contrast, in PiZ mice receiving rAAV-ZFN (groups 2–5), without (group 3) or with (group 5) rAAV-TI, Gli2 content was significantly reduced ($p < 0.02$).

rAAV-ZFN therapy reduced hepatic TIMP-1

The degradation of matrix proteins is mediated by matrix metalloproteinases, which are regulated by endogenous TIMPs.[19,25,26] Western blot analysis showed that hepatic TIMP-1 content was significantly higher in control 30-week-old PiZ mice than in age-matched C57/Bl6 mice (Figure 6C, D). TIMP-1 levels were reduced 6 months after treatment with high doses of rAAV-ZFN pair with (group 5) or without (group 3) the rAAV-TI ($p < 0.01$) (Figure 6C, D).

Serological analysis showed no evidence of liver injury 6 months after rAAV injections

Serum bilirubin, albumin, and alanine aminotransferase levels in all experimental mouse groups were found to be within normal range.

DISCUSSION

Our results show that ZFN expression in hepatocytes of PiZ mice through i.v. administration of an rAAV pair resulted in targeted disruption (*indel*) of the *SA1-ATZ* transgene by NHEJ. In this study, we used ZFN packaged into AAV2/8 for systemic delivery. ZFNs were chosen over CRISPR-Cas for *in vivo* gene editing because the small AAV genome would not accommodate Cas9 DNA along with the liver-specific promoter, polyA, and the gRNA expression cassette. Two weeks after injection, which is near the peak time point of rAAV2/8-mediated transgene expression in mouse

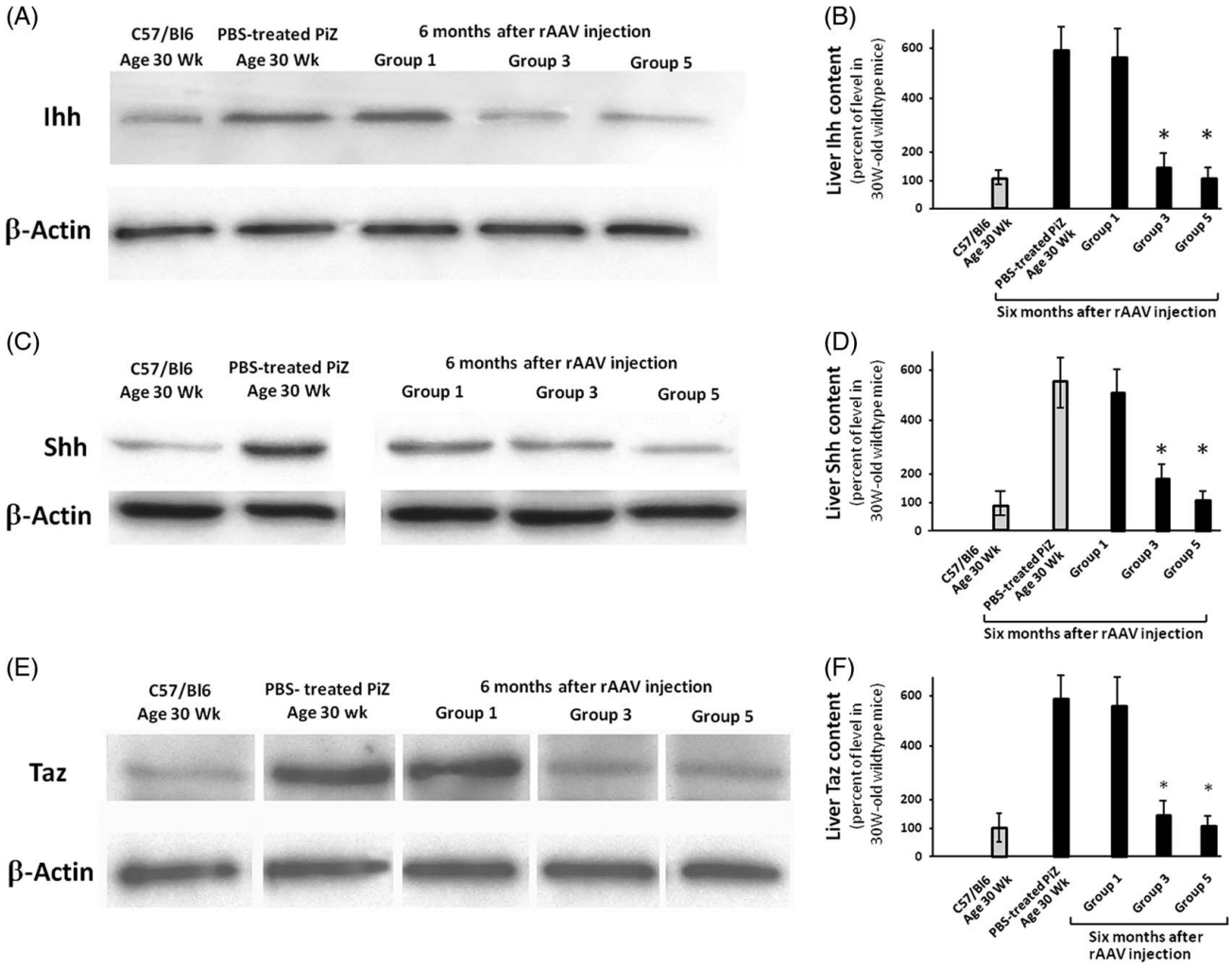

FIGURE 5 Hepatic Ihh, Shh, and TAZ (WWTR1) content: representative western blots for Ihh (A), Shh (C), and TAZ/WWTR1 (E), along with β-actin as loading control are shown for group 1 (rAAV-TI only), group 3 (rAAV-ZFN HD), group 5 (rAAV-ZFN HD + rAAV-TI), and PBS-injected control PiZ mice at the 6 month time point after injection. Liver from an age-matched wild-type C57/Bl6 mouse is also shown. Hepatic contents of Ihh (B), Shh (D), and TAZ/WWTR1 (F), as well as β-actin were determined by scanning the western blot bands and are shown as percentage of the protein content in 30-week-old wild-type C57/Bl6 mouse livers (means ± SEM, 6 mice in each group). *Significantly different from values in PBS-injected PiZ mice 6 months after injection, $p < 0.02$). Abbreviations: Ihh, Indian hedgehog; rAAV, recombinant adeno-associated viruses; Shh, sonic hedgehog.

hepatocytes, deep sequencing showed that the fraction of *SA1-ATZ* transgenes in the liver that had undergone disruption was modest but dose related. Six months after the administration of the rAAVs, the *indel*-containing fraction of SA1-ATZ increased 3- to 6-fold over the values at the 2-week time point, suggesting progressive repopulation of the liver by hepatocytes that had undergone gene disruption. However, although the trend was obvious, there was a marked variation of the effect among the PiZ mice in both low-dose and high-dose groups, so that statistical significance was not reached. Notably, the rAAV vectors were designed to express ZFNs from a hepatocyte-specific promoter, whereby nonparenchymal cells that contribute 40% of the hepatic genomic pool would not be expected to undergo NHEJ. Therefore, in an additional group of mice, we isolated hepatocytes from the livers of PiZ mice by collagenase perfusion and purification by differential centrifugation 6 months after ZFN-rAAV injection, followed by deep sequencing. Hepatocytes isolated from mice that had received rAAV-TI only showed a very low level of SA1-TI genome editing (NHEJ or TI). In contrast, in all rAAV-ZFN-treated groups, a high level of *indel*s (60%–70%) was observed ($p < 0.02$, compared with the rAAV-TI group). Correction of the *SA1-ATZ* transgenes by TI was observed only in the groups that had received rAAV-TI, in addition to rAAV-ZFN. Levels of TI in the total liver gene pool were very low 2 weeks after rAAV-ZFN plus rAAV-TI administration, an average of 10% and 30% of the *SA1-ATZ* transgene exhibited gene correction 6 months after treatment with the low dose and HD of rAAV-ZFN, respectively. Taken together, these results indicate that a relatively small number of hepatocytes that were

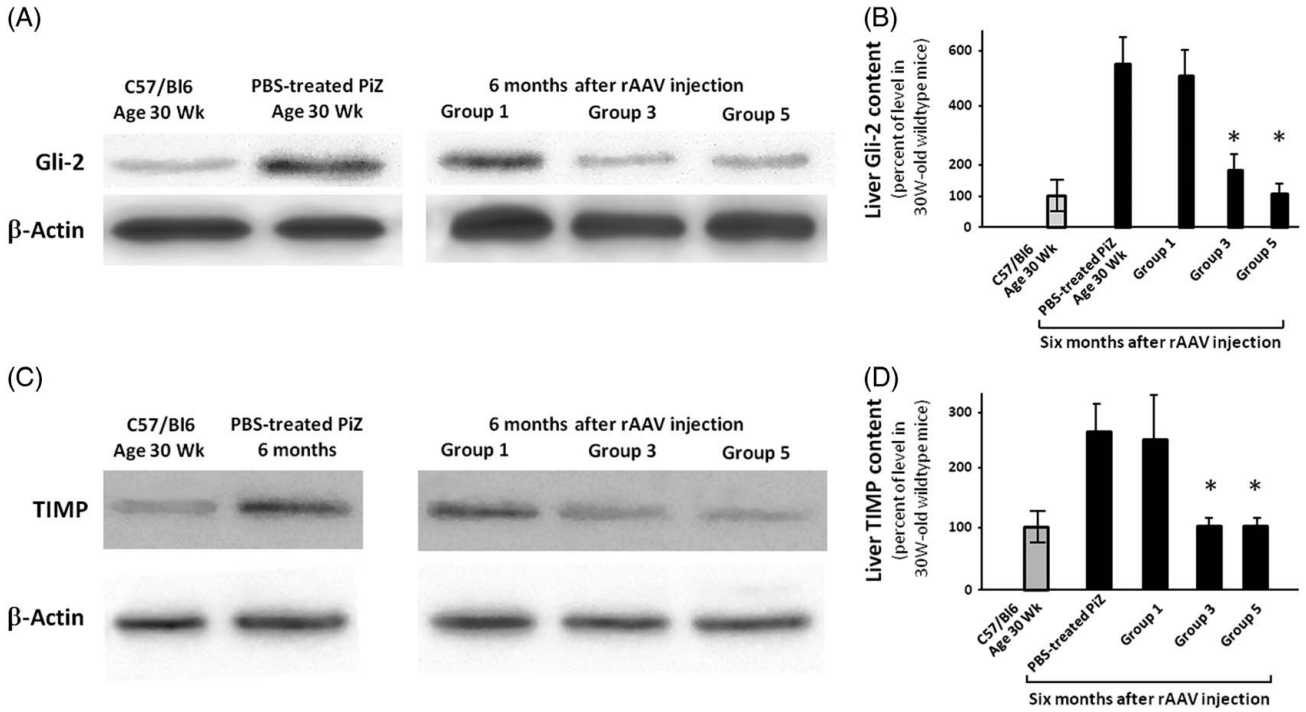

FIGURE 6 Hepatic Gli2 and TIMP content: representative western blots for Gli2 (6A) and TIMP (6C), along with β-actin as loading control are shown for group 1 (rAAV-TI only), group 3 (rAAV-ZFN HD), group 5 (rAAV-ZFN HD + rAAV-TI), and PBS-injected PiZ mice 6 months after injection. Liver from an age-matched wild-type C57/Bl6 mouse is also shown. Hepatic Gli2 (6B) and TIMP (6D) contents were determined by scanning the western blot bands and are shown as percentage of the Gli2 and TIMP content in 30-week-old wild-type C57/Bl6 mouse livers (means ± SEM, 6 mice in each group). *Significantly different from values in PBS-injected PiZ mice 6 months after injection, $p < 0.02$). Abbreviation: Gli2, glioblastoma-2; rAAV, recombinant adeno-associated viruses.

initially relieved of misfolded ATZ burden through *SA1-ATZ* transgene disruption underwent preferential proliferation over the ATZ-expressing native hepatocytes, leading to progressive liver repopulation by the gene-edited hepatocytes. This is consistent with our previous demonstration that wild-type mouse hepatocytes transplanted into PiZ mouse livers spontaneously repopulated the liver over time.[11] Similarly, Borel et al[13] found that wild-type human hepatocytes transplanted into the livers of immune-deficient PiZ mice, as well as endogenous mouse hepatocytes expressing a synthetic miRNA to silence the *SA1-ATZ* transgene through integration into the albumin locus provided a selective advantage over the endogenous PiZ hepatocytes. Notably, despite the hepatocellular stress caused by *SI-ATZ* expression, PiZ mouse hepatocytes are capable of surviving, proliferating and maintaining the liver mass.[12] However, when wild-type hepatocytes are transplanted into PiZ livers, the engrafted cells proliferate by replacing the ATZ-stressed host hepatocytes without increasing the liver mass. Such context-dependent cell elimination through short-range cell-cell interaction, which enables cells with higher fitness to replace neighboring less-fit cells, has been termed cell competition. The mechanisms of cell competition include signaling imbalances between distinct cells within a given cell population and the mechanical consequences of differential growth rates.[27] In our present study, the liver weight to body weight ratio remained unchanged despite a marked increase in the proportion of *SA1-ATZ*-disrupted hepatocytes, which is consistent with liver repopulation through cell competition.

Next, we compared the proportion of hepatocytes that contained polymerized ATZ globules at 2 weeks and 6 months after gene editing. In 6-week-old untreated PiZ mice, a great majority of the hepatocytes contain globules of polymerized ATZ. The percentage of globule-containing hepatocytes decreases with age so that in 30-week-old PiZ mice, ~40% of the hepatocytes lack the ATZ globules. It should be noted that the nonglobule-containing hepatocytes continue to express ATZ, as shown by Laser dissection microscopy of PiZ mouse livers, followed by quantitative RT PCR.[11] Two weeks after rAAV-ZFN administration, with or without rAAV-TI, the percentage of globule-containing cells was similar to that in the age-matched untreated control. In contrast, there was a marked reduction in the percentage of globule-containing cells in all-treated groups that received rAAV-ZFN with or without rAAV-TI, consistent with liver repopulation by *SA1-ATZ* transgene-disrupted cells. A critical intracellular concentration of ATZ is required for globule formation, which may depend on various factors, including the autophagy of the mutant protein.[28] Thus, the lack of ATZ globules indicates reduction, but not necessarily the absence of *SA1-ATZ* transgene

expression. In parallel with the depletion of hepatocellular ATZ globules, there was a reduction of serum ATZ levels in the recipients of rAAV-ZFN 6 months after the administration of rAAV-ZFN, with or without rAAV-TI. A fraction of the serum human AAT could have been contributed by normal human ATM, as suggested by gene correction by TI that was found in some mice 6 months after the administration of rAAV-ZFN plus rAAV-TI, but we were not able to evaluate the presence of wild-type ATM in serum as no antibodies are available that distinguishes human ATM from ATZ.

In contrast to the percentage of globule-containing hepatocytes, which decreases with age, liver fibrosis progresses with the aging of the PiZ mice. Activated HSC are primarily responsible for producing collagen that polymerizes into fibrotic strands as a part of the repair mechanism after various types of liver injury. Crosstalk between liver parenchymal cells and HSCs, particularly through hedgehog signaling, has been demonstrated in several models of liver injury.[16,29,30] Of particular interest was the finding that upregulation of TAZ, which leads to increased expression of Ihh, resulted in the progression of nonalcoholic hepatic steatosis to NASH with fibrosis.[29,30] In PiZ mice, the initial stress caused by the accumulation of polymerized ATZ is limited to hepatocytes because among the different types of liver cells, the AAT promoter is active specifically in hepatocytes. Therefore, liver fibrosis that occurs with the increasing age of the PiZ mice is likely to be the consequence of hepatocyte-HSC crosstalk.

Toward elucidating the mechanism underlying the resolution of liver fibrosis, we tested the hypothesis that the resolution of liver fibrosis in PiZ mice after repopulation by *SI-ATZ*-disrupted hepatocytes involves hedgehog proteins secreted by hepatocytes stressed by ATZ load. Therefore, in addition to determining the effect of liver repopulation by the *SI-ATZ*-disrupted hepatocytes on liver hedgehog protein concentration, we also quantified the hepatic content of TAZ/WWTR1, which is upstream to hedgehog gene expression, as well as the glioma family of proteins that are downstream mediators of hedgehog signaling.

To limit the SI-ATZ transgene editing to hepatocytes, we used rAAV-ZFN, which expresses the ZFN pair from a hepatocyte-specific promoter. Hepatocytes relieved of the load of ATZ expanded in 6 months, largely by competitive replacement of the ATZ-stressed native hepatocyte population, as indicated by genomic analysis. In parallel with liver repopulation by *SI-ATZ*-disrupted hepatocytes, there was a significant reduction of TAZ, Ihh, and Shh content of the liver, culminating in the reduction of gli1 and TIMP content and consequent resolution of the fibrosis. The resolution of fibrosis was observed by 2 histological staining methods, Sirius red and Masson trichrome, as well as by western blot analysis of collagen-1. Along with the resolutions of the collagen strands, the areas suggestive of regenerative nodules were no longer detectable. Notably, this effect occurred with or without rAAV-TI but not in the group that received rAAV-TI alone.

Fibrosis and its resolution depend on the balance between matrix metalloproteinases, which degrade matrix proteins, and their pseudosubstrate inhibitors, termed tissue inhibitors of TIMPs. Of the 4 members of the TIMP family, TIMP-1 is considered to be the most important in liver fibrosis.[15] Although TIMP-1 does not initiate liver fibrosis by itself, increased TIMP-1 levels in the liver promotes fibrosis caused by hepatocellular injury or stress.[16] In an animal model, the reduction of hepatic TIMP expression was found to be a mechanism of the resolution of liver fibrosis.[17] Consistent with this, in our study, the marked reduction of hepatic TIMP-1 paralleled the reduction of fibrosis in PiZ mouse groups that received rAAV-ZFN.

Hedgehog is an evolutionarily conserved signaling pathway that has been shown to play an important role in initiating and maintaining liver fibrosis in a number of metabolic, toxic, and inflammatory diseases of the liver.[31–33] Sustained Hh signaling is needed for maintaining expanded populations of liver myofibroblasts for THE continuation of liver fibrosis. Of the 3 members of the mammalian hedgehog protein family, Shh and Indian hedgehog (Ihh) have been studied most extensively.[16] Hedgehog induces glycolytic metabolism in HSCs, leading to lactate accumulation, which reprograms the gene expression profile, resulting in their transition to myofibroblasts.[31] High proliferative and fibrogenic activities of myofibroblasts is central to excess collagen deposition in the liver. We show that hepatic Ihh and Shh contents in 30-week-old PiZ mice were at an average 4- to 6-fold higher than those in age-matched wild-type controls. In 30-week-old PiZ mice that had received HD rAAV-ZFN without (group 3) or with rAAV-TI 6 months before analysis, Ihh and Shh levels had decreased to nearly the levels in age-matched wild-type mice. It should be noted that various liver cell types, including hepatocytes, bile duct epithelia, HSCs, and hepatic sinusoidal endothelial cells express hedgehog proteins when under stress. As western blot analysis was performed in this study on whole liver homogenates, the results do not definitively indicate cell type-specific origin of the increased Ihh and Shh ligands. However, as the *SA1-ATZ* transgene expression is hepatocyte restricted, it is likely that hepatocytes were the site of increased hedgehog protein production. This is supported by the demonstration of hedgehog protein in hepatocytes in liver biopsy of human patients with α1-antitrypsin deficiency.[32] Hedgehog signaling in the target cells, such as HSCs is mediated by the glioma-associated oncogene family of proteins (Gli), which undergo stabilization and nuclear translocation on hedgehog signaling.[16,17] In the present study, Gli2 content in liver homogenates paralleled the concentration of the hedgehog ligands.

Our findings indicate that amelioration of the proteotoxic load by indels generated in the *SA1-ATZ* transgene is sufficient for liver repopulation by the gene-edited cells and consequent reversal of liver pathology, and this process does not require gene correction. This finding is consistent with the observation that degradation of the ATZ content of the liver of PiZ mice by pharmacological enhancement of autophagy resulted in reduction of hepatic fibrosis.[28] The PiZ mouse used in our study is not a model for lung disease caused by α1-antitrypsin deficiency, because of the presence of normal mouse α1-antitrypsin. Also, the anti-human AAT antibody used in this study does not distinguish between the normal ATM and disease causing ATZ. However, 6 months after treatment, in the group receiving HD of rAAV-ZFN plus rAAV-TI, about one third of the *SA1-ATZ* transgenes had undergone conversion to *SA1-ATM* by targeted insertion. This suggests that with further optimization of targeted insertion, ZFN-mediated gene editing of hepatocytes could result in plasma levels of ATM that would be sufficient to protect the lungs, preventing the progression of the pulmonary manifestation of human ATD. Although the CRISPR-Cas9 system is easier to produce in many research laboratories, the advantage of using ZFN include smaller packaging space needed and no requirement for a protospacer adjacent motif (PAM) in the genomic DNA downstream to the desired cut site, which limits the choice of DNA break sites for a given Cas nuclease.[34]

In summary, we show that a small percentage of hepatocytes in the PiZ mouse livers underwent genome editing in the SA-ATZ transgene through NHEJ or TI 2 weeks after rAAV-ZFN administration. Percentage of the gene-edited hepatocytes increased over 6 months by the preferential proliferation of the transgene-disrupted hepatocytes (NHEJ). When rAAV-TI was added to the rAAV-ZFN, gene correction occurred at a much lower frequency than indels. The percentage of the gene-corrected hepatocytes increased in proportion to the increase in indels. The treatment resulted in a marked reduction in the proportion of ATZ globule-containing hepatocytes and a resolution of liver fibrosis and collagen content. This was paralleled by a decrease in the hepatic concentration of hedgehog proteins (Ihh and Shh) and their upstream inducer TAZ/WWTR1, as well as Gli2 and TIMP, which are downstream mediators of hedgehog signaling in HSCs that culminates in increased collagen deposit in the liver. The results warrant further investigation of ZFN-mediated disruption of mutant SERPINA1 for treatment of the hepatic manifestations of ATD, even after the onset of liver fibrosis.

FUNDING INFORMATION

A research grant from Sangamo Therapeutics to Jayanta Roy-Chowdhury, P30DK41296 to Jayanta Roy-Chowdhury, RO1 DK092469 to Namita Roy-Chowdhury.

CONFLICT OF INTEREST

Ira J. Fox consults for Miromatrix and received grants from Von Bear Wolf and Pittsburgh ReLiver. Kenneth Kim, Matthew Mendel, Gregory J. Cost, and Anthony Conway are or were employees of Sangamo Therapeutics. The remaining authors have no conflicts to report.

REFERENCES

1. Rudnick DA, Perlmutter DH. α1-antitrypsin deficiency. In: Arias IM Alter HJ Boyer JL Cohen DE Shafritz DA Thorgeirsson SS Wolkoff AA, eds. Liver Biology and Pathobiology, 6th ed. John Wiley & Sons ; 2020:645–58.
2. de Serres FJ. Worldwide racial and ethnic distribution of alpha1-antitrypsin deficiency: summary of an analysis of published genetic epidemiologic surveys. Chest. 2002;122:1818–29.
3. Carel RW, Lomas DA. Conformational disease. Lancet. 1997; 350:134–8.
4. Crystal RG. 1-Antitrypsin deficiency, emphysema and liver disease: genetic basis and strategies for therapy. J Clin Invest. 1990;85:1343–52.
5. Mostafavi B, Diaz S, Tanash HA, Pitulainen E. Liver function in alpha-1 antitrypsin deficient individuals at 37-40 years of age. Medicine (Baltimore). 2017;96:e6180.
6. Chu AS, Chopra KB, Perlmutter DH. Is severe progressive liver disease caused by alpha-1 antitrypsin deficiency more common in children or adults? Liver Transpl. 2016;22:886–94.
7. Dirksen A, Dirksen A, Dijkman JH, Madsen, Stoel B, Hutchinson DCS, et al. A randomized clinical trial of alpha(1)-antitrypsin augmentation therapy. Am J Respir Crit Care Med. 1999;160: 1468–72.
8. Squires JE, Soltys KA, McKiernan P, Squires RH, Strom SC, Fox IJ, et al. Clinical hepatocyte transplantation: what is next? Curr Transplant Rep. 2017;4:8280–289.
9. Shafritz DA, Grompe M. (2020) Liver repopulation by cell transplantation and the role of stem cells in liver biology. In: Arias IM Alter HJ Boyer JL Cohen DE Shafritz DA Thorgeirsson SS Wolkoff AA, eds. Liver Biology and Pathobiology, 6th ed. John Wiley & Sons ; 2020:6550–565.
10. Joseph B, Kapoor S, Schilsky ML, Gupta S. Bile salt–induced pro-oxidant liver damage promotes transplanted cell proliferation for correcting Wilson disease in the Long-Evans Cinnamon rat model. Hepatology. 2009;49:1616–24.
11. Ding J, Yannam GR, Roy-Chowdhury N, Hidvegi T, Basma H, Rennard SI, et al. Spontaneous hepatic repopulation in transgenic mice expressing mutant human a1-antitrypsin by wildtype donor hepatocytes. J Clin Invest. 2011;121:1930–4.
12. Rudnick DA, Liao Y, An J-K, Muglia LJ, Perlmutter DH, Teckman JH. Analyses of hepatocellular proliferation in a mouse model of α-1-antitrypsin deficiency. Hepatology. 2004;39:1048–55.
13. Borel F, Tang Q, Gernoux G, Greer C, Wang Z, Barzel A, et al. Survival advantage of both human hepatocyte xenografts and genome-edited hepatocytes for treatment of α-1 antitrypsin deficiency. Mol Ther. 2017;25:2477–89.
14. Bjursell M, Porritt MJ, Ericson E, Taheri-Ghahfarokhi A, Clausena M, Magnusson L, et al. Therapeutic genome editing with CRISPR/Cas9 in a humanized mouse model ameliorates α1-antitrypsin deficiency phenotype. EBioMedicine. 2018;29: 104–1.
15. Shen S, Sanchez ME, Blomenkamp, Erik M, Corcoran EM, Marco E, et al. Amelioration of Alpha-1 antitrypsin deficiency diseases with genome editing in transgenic mice. Hum Gene Ther. 2017;29:861–73.
16. Omenetti A, Choi S, Michelotti G, Diehl AM. Hedgehog signaling in the liver. J Hepatol. 2011;54:366–73.

17. Jung Y, Witek RP, Syn WK, Choi SS, Omenetti A, Premont R, et al. Signals from dying hepatocytes trigger growth of liver progenitors. Gut. 2010;59:655–65.
18. Konishi T, Schuster RM, Lentsch AB. Proliferation of hepatic stellate cells, mediated by YAP and TAZ, contributes to liver repair and regeneration after liver ischemia-reperfusion injury. Am J Physiol Gastrointest Liver Physiol. 2018;314:G471–82.
19. Iredale JP, Benyon RC, Pickering J, McCullen M, Northrop M, Pawley S, et al. Mechanisms of spontaneous resolution of rat liver fibrosis. Hepatic stellate cell apoptosis and reduced hepatic expression of metalloproteinase inhibitors. J Clin Invest. 1998; 102:538–49.
20. Sifers RN, Carlson JA, Clift SM, DeMayo FJ, Bullock DW, Woo SLC. Tissue specific expression of the human alpha-1-antitrypsin gene in transgenic mice. Nucl Acids Res. 1987;15:1459–75.
21. Miao CH, Ohashi K, Patijn GA, Meuse L, Ye X, Thompson AR, et al. Inclusion of the hepatic locus control region, an intron, and untranslated region increases and stabilizes hepatic factor IX gene expression in vivo but not in vitro. Mol Ther, 20201:522–32.
22. Jendrassik L, Gróf UP. Vereinfachte photometrische methoden zur bestimmung des blutbilirubins. B Biochem Z. 1938;297:81.
23. Qizibash A, Young-Pong O. Alpha-1-antitrypsin liver disease: differential diagnosis of PAS-positive diastase-resistant globules in liver cells. Am J Clin Pathol. 1983;79:697–702; (1983).
24. Neufeld DS. Isolation of rat hepatocytes. Methods Mol Biol. 1997;75:145–51.
25. Murawaki Y, Ikuta Y, Idobe Y, Kitamura Y, Kawasaki H. Tissue inhibitor of metalloproteinase-1 in the liver of patients with chronic liver disease. J Hepatol. 1997;26:1213–9.
26. Yoshihi H, Kuriyama S, I Miamoto Y, Thorgeirsson UP, Gomez DE, Kawata M, et al. Tissue inhibitor of metalloproteinases-1 promotes liver fibrosis development in a transgenic mouse model. Hepatology. 2000;32:1248–54.
27. Baker NE. Emerging mechanisms of cell competition. Nature Reviews Genetics. 2020;21:683–97.
28. Hidvegi T, Ewing M, Hale P, Christine D, Beckett C, Kemp C, et al. An autophagy-enhancing drug promotes degradation of mutant alpha1-antitrypsin Z and reduces hepatic fibrosis. Science. 2010;329:229–32.
29. Wang X, Zheng Z, Caviglia JM, Corey KE, Herfel TM, Cai B, et al. Hepatocyte TAZ/WWTR1 promotes inflammation and fibrosis in nonalcoholic steatohepatitis. Cell Metab. 2016;24: 848–62.
30. Wang X, Sommerfeld MR, Jahn-Hofmann K, Cai B, Filliol A, Remotti HE, et al. A therapeutic silencing RNA targeting hepatocyte TAZ prevents and reverses fibrosis in nonalcoholic steatohepatitis in mice. Hepatol Commun 2019;3:1221–34.
31. Chen Y, Choi SS, Michelotti FA, Chan IS, Swiderska M, Karaca GF, et al. Hedgehog controls hepatic stellate cell fate by regulating metabolism. Gastroenterology. 2012;143:1319–29.
32. Rangwala F, Guy CD, Lu J, Suzuki A, Burchette JL, Abdelmalek MF, et al. Increased production of sonic hedgehog by ballooned hepatocytes. J Pathol. 2011;224:401–10.
33. Philips GM, Chan IS, Swiderska M, Schroder VT, Guy C, Karaca GF, et al. Hedgehog signaling antagonist promotes regression of both liver fibrosis and hepatocellular carcinoma in a murine model of primary liver cancer. PLoS One. 2011;6: e23943.
34. Mekler V, Kuznedelov K, Severinov K. Quantification of the affinities of CRISPR–Cas9 nucleases for cognate protospacer adjacent motif (PAM) sequences. JBiol Chem. 2020;295: 6509–17.

How to cite this article: Li Y, Guha C, Asp P, Wang X, Tchaikovskya TL, Kim K, et al. Resolution of hepatic fibrosis after ZFN-mediated gene editing in the PiZ mouse model of human α1-antitrypsin deficiency. Hepatol Commun. 2023;7: e0070. https://doi.org/10.1097/HC9.0000000000000070